Acoustic equations of state for simple lattice Boltzmann velocity sets

Erlend Magnus Viggen*

Acoustics Research Centre, Department of Electronics and Telecommunications, Norwegian University of Science and Technology, Trondheim, Norway and Acoustics Research Centre, SINTEF ICT, Trondheim, Norway

(Received 2 May 2014; published 31 July 2014)

The lattice Boltzmann (LB) method typically uses an isothermal equation of state. This is not sufficient to simulate a number of acoustic phenomena where the equation of state cannot be approximated as linear and constant. However, it is possible to implement variable equations of state by altering the LB equilibrium distribution. For simple velocity sets with velocity components $\xi_{i\alpha} \in \{-1,0,1\}$ for all i, these equilibria necessarily cause error terms in the momentum equation. These error terms are shown to be either correctable or negligible at the cost of further weakening the compressibility. For the D1Q3 velocity set, such an equilibrium distribution is found and shown to be unique. Its sound propagation properties are found for both forced and free waves, with some generality beyond D1Q3. Finally, this equilibrium distribution is applied to a nonlinear acoustics simulation where both mechanisms of nonlinearity are simulated with good results. This represents an improvement on previous such simulations and proves that the compressibility of the method is still sufficiently strong even for nonlinear acoustics.

DOI: 10.1103/PhysRevE.90.013310 PACS number(s): 47.11.−j, 43.25.−x

I. INTRODUCTION

In a fluid, the ideal speed of sound c is directly dependent on the fluid's equation of state as

$$c^2 = \left(\frac{\partial p}{\partial \rho}\right)_s, \tag{1}$$

where p is the pressure, ρ is the density, and the entropy s is held constant [1,2]. This speed of sound is typically evaluated at a rest state that represents, e.g., undisturbed atmospheric conditions in air. This rest state is characterized by a pressure p_0 and a density ρ_0 and the result is the small-signal ideal speed of sound c_0.

For gases that are ideal or nearly so, the speed of sound can be calculated from the isentropic adiabatic equation of state [1,2]

$$\frac{p}{p_0} = \left(\frac{\rho}{\rho_0}\right)^\gamma \overset{(1)}{\Rightarrow} c^2 = c_0^2\left(\frac{\rho}{\rho_0}\right)^{\gamma-1}, \qquad c_0^2 = \gamma p_0/\rho_0. \tag{2}$$

Here γ is the specific heat ratio, also known as the adiabatic index. Its maximum is $\gamma = 5/3$ for a monatomic gas and its minimum is $\gamma = 1$ for an isothermal gas. In the latter case, the equation of state becomes linear and the speed of sound becomes constant $c = c_0$.

The virtual fluid simulated by basic lattice Boltzmann (LB) models [3,4] has such a linear isothermal equation of state $p = c_{\mathrm{vs}}^2\rho$, with c_{vs} being a model constant. While this equation of state does not correspond to any physical fluid, it is still quite flexible. For small disturbances, more general equations of state can be linearized as [1,2]

$$p = p_0 + p' \simeq p_0 + c_0^2\rho', \tag{3}$$

where $p' = p - p_0$ and $\rho' = \rho - \rho_0$ represent deviations from the rest state and p_0 and c_0 can be a function of space and time. Since the fluid mass and momentum conservation equations only contain pressure through a pressure gradient term $\nabla p = \nabla p'$, the rest pressure p_0 does not affect these equations. While p_0 does matter in the energy conservation equation, this equation is not relevant in nonthermal lattice Boltzmann models. Consequently, if we are only interested in the evolution of density and momentum, we need only consider the pressure fluctuation's equation of state $p' = c_0^2\rho'$, which can be perfectly captured by the isothermal LB equation of state if c_0 is a constant.

However, the isothermal equation of state is not as useful in cases where the equation of state cannot be approximated as being linear and constant. If we could choose the simulated equation of state more freely, we would be able to simulate acoustic phenomena that cannot be simulated with the isothermal equation of state. For example, fully nonlinear acoustics requires a nonlinear equation of state, refraction requires a spatially varying equation of state, and the nonequilibrium phenomenon of molecular relaxation requires a time-dependent equation of state. The latter is by far the dominant sound absorption mechanism in air at audible frequencies [2,5]. A more flexible equation of state could also be dependent on underlying variables, such as a thermal field evolved with a connected advection-diffusion scheme, which would also allow capturing the sound wave absorption caused by thermal conduction.

In pseudopotential multiphase and multicomponent LB models [6–8], the equation of state is altered by adding a body force. In each node, this force depends on the density of each component in the node itself and its neighboring nodes through mesoscopic interparticle potentials. However, this application is a very different one from acoustics.

In this article we look at how acoustic equations of state may be implemented through the LB equilibrium distribution. While there are many possible such implementations, we here look at common features of all such equilibria for simple velocity sets, where all the nonzero velocities fall on a single d cube in $1 \leqslant d \leqslant 3$ spatial dimensions.

*erlendmagnus.viggen@sintef.no

Section II gives an overview of relevant aspects of the lattice Boltzmann method. Section III briefly reviews the requirements on equilibrium distributions with arbitrary equations of state and how these requirements can only be approximated using simple velocity sets, resulting in approximation errors. It subsequently shows that these errors are not too severe and derives a unique D1Q3 equilibrium that is the one-dimensional projection of all such higher-dimensional equilibria. (The analysis of this equilibrium therefore has some generality to these higher-dimensional equilibria.) In Sec. IV a standard linearization analysis is performed on this equilibrium to determine its linear sound propagation properties. The results of Secs. III and IV are used in Sec. V to perform an LB simulation of fully nonlinear acoustics, which is an improvement over the partially nonlinear LB acoustics simulations previously shown in the literature [9,10].

II. LATTICE BOLTZMANN METHOD

The fundamental variable in the lattice Boltzmann method is the distribution function $f_i(\mathbf{x},t)$, which represents the density of particles with velocity $\boldsymbol{\xi}_i$ at point $\mathbf{x}$ and time t. The particle velocities $\boldsymbol{\xi}_i$ and their matching weighting coefficients w_i are limited to a small discrete set. The aforementioned simple velocity sets are listed for one to three dimensions in the literature [11]. These velocity sets all fulfill the isotropy conditions [12]

$$\sum_i w_i = 1, \tag{4a}$$

$$\sum_i w_i \xi_{i\alpha} = 0, \tag{4b}$$

$$\sum_i w_i \xi_{i\alpha}\xi_{i\beta} = c_{\mathrm{vs}}^2 \delta_{\alpha\beta}, \tag{4c}$$

$$\sum_i w_i \xi_{i\alpha}\xi_{i\beta}\xi_{i\gamma} = 0, \tag{4d}$$

$$\sum_i w_i \xi_{i\alpha}\xi_{i\beta}\xi_{i\gamma}\xi_{i\delta} = c_{\mathrm{vs}}^2(\delta_{\alpha\beta}\delta_{\gamma\delta} + \delta_{\alpha\gamma}\delta_{\beta\delta} + \delta_{\alpha\delta}\delta_{\beta\gamma}), \tag{4e}$$

$$\sum_i w_i \xi_{i\alpha}\xi_{i\beta}\xi_{i\gamma}\xi_{i\delta}\xi_{i\epsilon} = 0, \tag{4f}$$

where c_{vs} is a velocity set constant that equals $1/\sqrt{3}$ for these velocity sets and $\delta_{\alpha\beta}$ is the Kronecker delta. Generic Cartesian indices for which the Einstein summation convention is used are labeled with Greek letters. We employ simplified lattice units with normalized space and time resolution $\Delta x = \Delta t = 1$ throughout this article except in Sec. V.

The macroscopic quantities of density $\rho(\mathbf{x},t)$ and fluid velocity $\mathbf{u}(\mathbf{x},t)$ can be found as moments of f_i,

$$\rho = \sum_i f_i = \Pi_0, \quad \rho u_\alpha = \sum_i \xi_{i\alpha} f_i = \Pi_\alpha. \tag{5a}$$

In addition, we will later have use for the higher-order moments

$$\sum_i \xi_{i\alpha}\xi_{i\beta} f_i = \Pi_{\alpha\beta}, \quad \sum_i \xi_{i\alpha}\xi_{i\beta}\xi_{i\gamma} f_i = \Pi_{\alpha\beta\gamma}. \tag{5b}$$

The evolution of f_i is determined by the lattice Boltzmann equation

$$f_i(\mathbf{x}+\boldsymbol{\xi}_i, t+1) - f_i(\mathbf{x},t) = \Omega\big[f_i(\mathbf{x},t), f_i^{(0)}(\mathbf{x},t)\big], \tag{6}$$

where the right-hand side is a collision operator that relaxes the local distribution function $f_i(\mathbf{x},t)$ towards a local equilibrium distribution $f_i^{(0)}(\mathbf{x},t)$. The simplest collision operator that results in correct conservation of mass and momentum is the Bhatnagar-Gross-Krook (BGK) operator where all the distribution functions f_i are relaxed directly towards $f_i^{(0)}$ with the same relaxation time τ,

$$\Omega\big[f_i(\mathbf{x},t), f_i^{(0)}(\mathbf{x},t)\big] = -\frac{1}{\tau}\big[f_i(\mathbf{x},t) - f_i^{(0)}(\mathbf{x},t)\big]. \tag{7}$$

The equilibrium distribution is constructed from the moments of f_i. A widely used choice is the isothermal equilibrium [11]

$$f_i^{(0)} = \rho w_i\left(1 + \frac{\boldsymbol{\xi}_i\cdot\mathbf{u}}{c_{\mathrm{vs}}^2} + \frac{(\boldsymbol{\xi}_i\cdot\mathbf{u})^2}{2c_{\mathrm{vs}}^4} - \frac{\mathbf{u}\cdot\mathbf{u}}{2c_{\mathrm{vs}}^2}\right). \tag{8}$$

This is arguably the most stable choice for an isothermal equilibrium polynomial truncated to $O(u^2)$ [13].

It is far from obvious that this simple mesoscopic numerical scheme leads to the correct macroscopic behavior. This is proven from a Taylor expansion of (6) and a subsequent Chapman-Enskog perturbation analysis where f_i and its derivatives are expanded in a parameter ϵ, which labels each term's order of smallness [3,4,12]. The expanded forms are

$$f_i = f_i^{(0)} + \epsilon f_i^{(1)} + \epsilon^2 f_i^{(2)} + \cdots,$$
$$\frac{\partial}{\partial t} = \epsilon\frac{\partial^{(1)}}{\partial t} + \epsilon^2\frac{\partial^{(2)}}{\partial t} + \cdots, \quad \nabla = \epsilon\nabla^{(1)}.$$

At the lowest order in ϵ, the moments of the $(\partial^{(1)}/\partial t + \boldsymbol{\xi}_i\cdot\nabla^{(1)})f_i^{(0)}$ term results in the Euler-level fluid equations. At the next order in ϵ, the moments of the $\partial^{(2)} f_i^{(0)}/\partial t$ and $(\partial^{(1)}/\partial t + \boldsymbol{\xi}_i\cdot\nabla^{(1)})f_i^{(1)}$ terms result in the Navier-Stokes-level corrections [4].

Assuming that the second moment is relaxed towards its equilibrium $\Pi_{\alpha\beta}^{(0)}$ with a relaxation time τ, the analysis shows that (6) is consistent with the macroscopic mass and momentum conservation equations

$$\frac{\partial\rho}{\partial t} + \frac{\partial\rho u_\alpha}{\partial x_\alpha} = 0, \tag{9a}$$

$$\frac{\partial\rho u_\alpha}{\partial t} + \frac{\partial}{\partial x_\beta}\left[\Pi_{\alpha\beta}^{(0)} + \left(1 - \frac{1}{2\tau}\right)\epsilon\Pi_{\alpha\beta}^{(1)}\right] = 0, \tag{9b}$$

where $\Pi_{\alpha\beta}^{(n)} = \sum_i \xi_{i\alpha}\xi_{i\beta} f_i^{(n)}$. The equilibrium moment $\Pi_{\alpha\beta}^{(0)}$ can be directly found from the equilibrium distribution $f_i^{(0)}$ using the isotropy conditions (4). To recover correct Euler-level terms in the momentum equation, $f_i^{(0)}$ must be chosen so that

$$\Pi_{\alpha\beta}^{(0)} = p\delta_{\alpha\beta} + \rho u_\alpha u_\beta. \tag{9c}$$

As an example, taking the second moment of (8) and using the isotropy conditions (4), we find (9c) with an isothermal equation of state $p = c_{\mathrm{vs}}^2\rho$.

With this expression for $\Pi_{\alpha\beta}^{(0)}$, it is clear that $\Pi_{\alpha\beta}^{(1)}$ must be related to the stress tensor. From the Chapman-Enskog analysis

[4], we know that it is generally determined as

$$\Pi^{(1)}_{\alpha\beta} = -\tau\left[\frac{\partial^{(1)}\Pi^{(0)}_{\alpha\beta}}{\partial t} + \frac{\partial^{(1)}\Pi^{(0)}_{\alpha\beta\gamma}}{\partial x_\gamma}\right]. \tag{9d}$$

Consequently, we know that $f_i^{(0)}$ determines the resulting momentum equation, both directly through $\Pi^{(0)}_{\alpha\beta}$ and indirectly through $\Pi^{(1)}_{\alpha\beta}$.

Now, how can the simulation's equation of state and sound speed be made variable? One method is to keep the isothermal equilibrium distribution (8) and add body forces $\mathbf{F} \propto \nabla\rho$ to the model to augment the isothermal pressure gradient $c_{\mathrm{vs}}^2\nabla\rho$ [10,14]. However, this method requires the use of a finite-difference scheme or a similar method to determine $\nabla\rho$, which causes its own accuracy problems and makes boundary conditions more difficult to handle. In addition, this method has no clear physical interpretation.

Alternatively, we can choose a more general equilibrium distribution $f_i^{(0)}$ where we can directly specify the pressure p. In these models, lower pressures correspond to a larger ratio of rest particles, giving a physically correct lower average particle speed. Indeed, many such equilibrium distributions have been proposed [7,15–19].

However, the stability of such equilibria is a complicated topic: Even equilibria that result in correct macroscopic equations may result in unstable simulations for certain velocity sets. As an example, stability for the D2Q9 velocity set requires a particular choice of a nonhydrodynamic moment of the equilibrium distribution [19]. We will now consider such equilibrium distributions further, regarding the velocity set-specific topic of stability as being beyond the scope of this article.

III. GENERALIZED EQUILIBRIUM DISTRIBUTION

How then should the equilibrium distribution $f_i^{(0)}$ be chosen? To recover an ideal momentum equation, the moments of $f_i^{(0)}$ must be

$$\Pi^{(0)}_0 = \sum_i f_i^{(0)} = \rho, \tag{10a}$$

$$\Pi^{(0)}_\alpha = \sum_i \xi_{i\alpha} f_i^{(0)} = \rho u_\alpha, \tag{10b}$$

$$\Pi^{(0)}_{\alpha\beta} = \sum_i \xi_{i\alpha}\xi_{i\beta} f_i^{(0)} = p\delta_{\alpha\beta} + \rho u_\alpha u_\beta, \tag{10c}$$

$$\Pi^{(0)}_{\alpha\beta\gamma} = \sum_i \xi_{i\alpha}\xi_{i\beta}\xi_{i\gamma} f_i^{(0)} = p(u_\alpha\delta_{\beta\gamma} + u_\beta\delta_{\alpha\gamma} + u_\gamma\delta_{\alpha\beta}) + \rho u_\alpha u_\beta u_\gamma. \tag{10d}$$

As we saw in the previous section, the higher-order moments have no effect on the macroscopic behavior at the Navier-Stokes level. From (9), these choices would result in a momentum equation

$$\frac{\partial\rho u_\alpha}{\partial t} + \frac{\partial\rho u_\alpha u_\beta}{\partial x_\beta} = -\frac{\partial p}{\partial x_\alpha} + p\left(\tau - \frac{1}{2}\right)\frac{\partial}{\partial x_\beta} \times\left[\frac{\partial u_\alpha}{\partial x_\beta} + \frac{\partial u_\beta}{\partial x_\alpha} + \left(1 - \frac{\rho c^2}{p}\right)\delta_{\alpha\beta}\frac{\partial u_\gamma}{\partial x_\gamma}\right]. \tag{11}$$

In deriving this equation we have assumed that $p = p(\rho,s)$ and that $\partial^{(1)}s/\partial t = 0$. The former assumption is an expression of the state principle of equilibrium thermodynamics [1]. The latter assumption is justified by the $\partial^{(1)}/\partial t$ derivative being connected to the Euler equations [4], which are isentropic [5]. The speed of sound c is determined by the equation of state through (1).

In this momentum equation we have a dynamic shear viscosity $\mu = p(\tau - 1/2)$ and a dynamic bulk viscosity $\mu_{\mathrm{B}} = (5/3 - \rho c^2/p)\mu$. In the case of the isentropic equation of state (2), we may insert the linearized speed of sound $c_0^2 = \gamma p_0/\rho_0$ to find the linearized bulk viscosity $\mu_{\mathrm{B}} = (5/3 - \gamma)\mu$, which directly depends on the adiabatic index γ. This value has also been found from polyatomic kinetic theory in the limit of very rapid equilibration of inner energies [20]. In addition, this bulk viscosity has well-known limits: $\mu_{\mathrm{B}} = 0$ for a monatomic gas and $\mu_{\mathrm{B}} = 2\mu/3$ for an isothermal gas [4].

However, there is a linear dependence between the moments for all the simple cubic velocity sets. For instance,

$$\Pi^{(0)}_{xxx} = \sum_i \xi_{ix}\xi_{ix}\xi_{ix} f_i^{(0)} = \sum_i \xi_{ix} f_i^{(0)} = \Pi^{(0)}_x \tag{12}$$

since $\xi_{ix} \in \{-1,0,1\}$ for all i in these velocity sets. Consequently, all the moments (10) are not simultaneously attainable for simple velocity sets. While they can be attained for extended velocity sets with more velocities, these require more simulation time and undermine a major strength of the LB method by making its implementation more difficult, especially with regard to boundary conditions. However, we will see in the following that the penalty of using a simple velocity set and having an imperfect third moment is not too severe.

For the third moment to comply with dependence relations such as (12) while remaining isotropic, it can only be

$$\Pi^{(0)}_{\alpha\beta\gamma} = \sum_i \xi_{i\alpha}\xi_{i\beta}\xi_{i\gamma} f_i^{(0)} = \rho c_{\mathrm{vs}}^2(u_\alpha\delta_{\beta\gamma} + u_\beta\delta_{\alpha\gamma} + u_\gamma\delta_{\alpha\beta}). \tag{13}$$

This corresponds to an inconsistent choice of pressure: p in the second moment and ρc_{vs}^2 in the third. The Chapman-Enskog analysis now leads to a macroscopic momentum equation with a number of additional error terms

$$\frac{\partial\rho u_\alpha}{\partial t} + \frac{\partial\rho u_\alpha u_\beta}{\partial x_\beta} = -\frac{\partial p}{\partial x_\alpha} + \rho c_{\mathrm{vs}}^2\left(\tau - \frac{1}{2}\right)\frac{\partial}{\partial x_\beta}\left[\frac{\partial u_\alpha}{\partial x_\beta} + \frac{\partial u_\beta}{\partial x_\alpha} + \left(1 - \frac{c^2}{c_{\mathrm{vs}}^2}\right)\delta_{\alpha\beta}\frac{\partial u_\gamma}{\partial x_\gamma}\right] + \left(\tau - \frac{1}{2}\right)\frac{\partial}{\partial x_\beta}\left[(c_{\mathrm{vs}}^2 - c^2)\delta_{\alpha\beta}u_\gamma\frac{\partial\rho}{\partial x_\gamma} + \left(u_\alpha\frac{\partial}{\partial x_\beta} + u_\beta\frac{\partial}{\partial x_\alpha}\right)(\rho c_{\mathrm{vs}}^2 - p) - \frac{\partial\rho u_\alpha u_\beta u_\gamma}{\partial x_\gamma}\right]. \tag{14}$$

The lack of the $O(u^3)$ term in $\Pi^{(0)}_{\alpha\beta\gamma}$ leads to the $(\tau - 1/2)\partial(\rho u_\alpha u_\beta u_\gamma)/\partial x_\gamma$ error term, which is also present for isothermal LB models using the velocity sets considered here [4]. The other error terms in (14) are caused by the inconsistent pressure.

This momentum equation has a dynamic shear viscosity $\mu = \rho c_{\mathrm{vs}}^2(\tau - 1/2)$ and a dynamic bulk viscosity $\mu_{\mathrm{B}} = (5/3 - c^2/c_{\mathrm{vs}}^2)\mu$. While it is unphysical for the bulk viscosity to depend on c^2/c_{vs}^2, the bulk viscosity in LB simulations can be corrected [4,12,21]. Additionally, the bulk viscosity recovers its correct isentropic value if $c^2 = \gamma c_{\mathrm{vs}}^2$.

This momentum equation also contains other unwanted terms, which will now be argued to be negligible for weakly compressible flow. In acoustics, it is largely assumed that the fluid variables are small fluctuations over a constant rest state,

$$\begin{bmatrix} \rho(\mathbf{x},t) \\ \mathbf{u}(\mathbf{x},t) \\ p(\mathbf{x},t) \end{bmatrix} = \begin{bmatrix} \rho_0 \\ \mathbf{0} \\ p_0 \end{bmatrix} + \varepsilon \begin{bmatrix} \rho'(\mathbf{x},t) \\ \mathbf{u}'(\mathbf{x},t) \\ p'(\mathbf{x},t) \end{bmatrix}. \tag{15}$$

Here the macroscopic smallness parameter ε labels the fluctuation's order of smallness. In linear acoustics, terms above $O(\varepsilon)$ are neglected. In the momentum equation (14) the stress tensor on the first line is $O(\mu\varepsilon)$. The error terms on the second line are $O(\mu\varepsilon^2)$ and $O(\mu\varepsilon^3)$. The latter error term is commonly neglected and we will now also neglect the former error terms. Consequently, the compressibility of the LB method is weakened further than usual. Even so, neglecting these terms is analogous to the approximation scheme used when deriving the equations of nonlinear acoustics [22].

Problems that are essentially one dimensional, such as the propagation of plane waves, can be simulated using the D1Q3 velocity set given by the velocities $(\xi_-,\xi_0,\xi_+) = (-1,0,1)$ and the weighting coefficients $(w_-,w_0,w_+) = (1/6,2/3,1/6)$. This velocity set is the one-dimensional projection of all simple velocity sets in two and three dimensions. Indeed, sound propagation along the x or y axis for the D2Q9 velocity set is identical to sound propagation for the D1Q3 velocity set [23].

The D1Q3 velocity set has only three independent moments, as can be seen from the transformations

$$\begin{bmatrix} 1 & 1 & 1 \\ -1 & 0 & 1 \\ 1 & 0 & 1 \end{bmatrix} \begin{bmatrix} f_-^{(0)} \\ f_0^{(0)} \\ f_+^{(0)} \end{bmatrix} = \begin{bmatrix} \rho \\ \rho u \\ \Pi_{xx}^{(0)} \end{bmatrix},$$

$$\begin{bmatrix} f_-^{(0)} \\ f_0^{(0)} \\ f_+^{(0)} \end{bmatrix} = \begin{bmatrix} 0 & -\frac{1}{2} & \frac{1}{2} \\ 1 & 0 & -1 \\ 0 & \frac{1}{2} & \frac{1}{2} \end{bmatrix} \begin{bmatrix} \rho \\ \rho u \\ \Pi_{xx}^{(0)} \end{bmatrix}, \tag{16}$$

where the second transformation matrix is the inverse of the first. Thus, the D1Q3 equilibrium is fully determined by the zeroth to second moments. Consequently, all equilibrium distributions $f_i^{(0)}$ with a variable equation of state must be equal when applied to the D1Q3 velocity set. Indeed, we can construct this equilibrium directly from (10),

$$f_0^{(0)} = \rho - p - \rho uu, \quad f_\pm^{(0)} = \tfrac{1}{2}(p \pm \rho u + \rho uu). \tag{17}$$

Unlike the equilibrium in (8), which is valid for multiple velocity sets, the weighting coefficients w_i do not enter into this equilibrium as it has been derived specifically for the D1Q3 velocity set.

Neglecting terms of $O(\mu\varepsilon^2)$ and above, the momentum equation (14) in one-dimensional form becomes

$$\begin{aligned} \frac{\partial \rho u}{\partial t} + \frac{\partial \rho uu}{\partial x} &= -\frac{\partial p}{\partial x} + \rho c_{\mathrm{vs}}^2 \left(\tau - \frac{1}{2}\right)\left(3 - \frac{c^2}{c_{\mathrm{vs}}^2}\right)\frac{\partial u}{\partial x} \\ &= -\frac{\partial p}{\partial x} + \mu\left(\frac{4}{3} + \frac{\mu_{\mathrm{B}}}{\mu}\right)\frac{\partial u}{\partial x}. \end{aligned} \tag{18}$$

In one-dimensional problems there can be no shear strain and the shear and bulk viscosities appear only together in the sum $(4\mu/3 + \mu_{\mathrm{B}})$. The effect of viscosity on sound propagation is often represented through the viscous relaxation time

$$\tau_{\mathrm{v}} = \frac{\mu}{\rho c^2}\left(\frac{4}{3} + \frac{\mu_{\mathrm{B}}}{\mu}\right) \quad \text{such that } \tau = \frac{\tau_{\mathrm{v}}}{3c_{\mathrm{vs}}^2/c^2 - 1} + \frac{1}{2} \tag{19}$$

for our model.

IV. SOUND PROPAGATION PROPERTIES

The sound propagation properties of absorption and dispersion can be found for this general D1Q3 equilibrium distribution by performing a standard linearization analysis to find the dispersion relation [4,24,25]. From previous arguments, the analysis of this D1Q3 equilibrium will have validity for sound propagation along a main axis using similar equilibria for higher-dimensional simple velocity sets for which D1Q3 is the one-dimensional projection. However, this D1Q3 analysis cannot take into account the effect of sound propagation anisotropy, which must be mapped individually for different higher-dimensional velocity sets and equilibria.

Similarly to (15), all variables are assumed to be small fluctuations around a constant rest state. For a plane wave, the distribution function becomes

$$\begin{aligned} \hat{f}_i(x,t) &= F_i^{(0)} + \hat{f}_i'(x,t) = F_i^{(0)} + \hat{f}_i^\star e^{i(\hat{\omega}t - \hat{k}x)} \\ &= F_i^{(0)} + \hat{f}_i^\star e^{-\alpha_t t} e^{-\alpha_x x} e^{i(\omega t - kx)}, \end{aligned} \tag{20}$$

where carets indicate quantities in the complex exponential wave formulation and starred quantities indicate amplitudes. Here $F_i^{(0)}$ and $\hat{f}_i'(x,t)$ represent a constant rest state and a small fluctuation as in (15); $\hat{f}_i'$ is assumed to be on a harmonic plane-wave form with amplitude $\hat{f}_i^\star$. The angular frequency $\hat{\omega}$ and wave number $\hat{k}$ become complex due to dissipative effects in the fluid and have been split into real and imaginary parts

$$\hat{\omega} = \omega + i\alpha_t, \quad \hat{k} = k - i\alpha_x. \tag{21}$$

The imaginary parts are time and space absorption coefficients, while the real parts are related to dispersion; the linear speed of sound is $c = \omega/k$. In the limit where we have no dispersion, $k = k_0$, $\omega = \omega_0$, and $c_0 = \omega_0/k_0$.

Absorbed harmonic waves can be separated into two main types where the sound propagation properties for one type cannot in general be applied to the other [26]. Waves that are radiated by a source at a frequency ω_0, so-called forced waves, will be dissipated only with the distance to the source as $\hat{\omega} = \omega_0$. Free waves are conversely characterized by $\hat{k} = k_0$, having infinite extent and an amplitude that is constant in space and exponentially decreasing in time. Only forced sound waves are physically realizable, though free waves are very useful for

benchmarking due to their spatially periodic nature. The LB linearization results for forced plane waves can also be used to accurately predict the propagation of non-plane waves [25].

Using the linearized equation of state (3) we can find a linearized version of (17) split into constant and fluctuating parts

$$F_0^{(0)} = \rho_0 - p_0, \quad F_\pm^{(0)} = \tfrac{1}{2}p_0, \tag{22a}$$

$$\hat{f}_0^{\star(0)} = \left(1 - c_0^2\right)\hat{\rho}^\star, \quad \hat{f}_\pm^{\star(0)} = \tfrac{1}{2}\left(c_0^2\hat{\rho}^\star \pm \rho_0\hat{u}^\star\right). \tag{22b}$$

Following the linearization analysis process [4,24], we find an eigenvalue problem in the form

$$\hat{\mathsf{A}}\hat{\mathbf{f}}^\star = e^{i\hat{\omega}}\hat{\mathbf{f}}^\star, \tag{23}$$

with $\hat{\mathbf{f}}^\star = [\hat{f}_-^\star, \hat{f}_0^\star, \hat{f}_+^\star]^{\mathrm{T}}$ and

$$\hat{\mathsf{A}} = \begin{bmatrix} \left(1 - \frac{1-c_0^2}{2\tau}\right)e^{-i\hat{k}} & \frac{c_0^2}{2\tau}e^{-i\hat{k}} & -\frac{1-c_0^2}{2\tau}e^{-i\hat{k}} \\ \frac{1-c_0^2}{\tau} & 1 - \frac{c_0^2}{\tau} & \frac{1-c_0^2}{\tau} \\ -\frac{1-c_0^2}{2\tau}e^{i\hat{k}} & \frac{c_0^2}{2\tau}e^{i\hat{k}} & \left(1 - \frac{1-c_0^2}{2\tau}\right)e^{i\hat{k}} \end{bmatrix}.$$

Note that the rest pressure p_0 does not enter into this equation, which is reasonable considering the argument in Sec. I on its arbitrariness. Relating τ to τ_v as in (19), the characteristic polynomial gives us a dispersion relation

$$\det(\hat{\mathsf{A}} - \mathsf{I}e^{i\hat{\omega}}) = g(\hat{\omega},\hat{k},c_0,\tau_\mathrm{v}) = 0.$$

The full and explicit forms of this dispersion relation and the following forced and free wave solutions are too cumbersome to reproduce here, but can be found from (23) using a computer algebra system.

For forced waves, where $\hat{\omega} = \omega_0$, the dispersion relation can be solved for $\hat{k}/k_0$. Expressing it in the form of a series expansion in ω_0, which represents the discretization error, nested inside a series expansion in $\omega_0\tau_\mathrm{v}$, which represents the physical effect of viscosity on wave propagation [2,26], we find

$$\begin{aligned}\frac{\hat{k}}{k_0} &= 1 + \frac{\omega_0^2}{24}\left(\frac{1}{c_0^2} - 1\right) + \frac{\omega_0^4}{1920}\left(\frac{9}{c_0^4} - \frac{10}{c_0^2} + 1\right) + O\left(\omega_0^6\right) \\ &\quad - i\frac{1}{2}(\omega_0\tau_\mathrm{v})\left[1 + \frac{\omega_0^2}{24}\left(\frac{3}{c_0^2} + 1\right) + O\left(\omega_0^4\right)\right] \\ &\quad - (\omega_0\tau_\mathrm{v})^2\left[\frac{1}{8}\frac{c_0^2+3}{1-c_0^2} + O(\omega_0^2)\right] + O((\omega_0\tau_\mathrm{v})^3).\end{aligned} \tag{24}$$

In the $\omega_0 \to 0$ limit of no discretization error this series expansion reduces to the forced wave propagation properties of the underlying discrete-velocity Boltzmann equation (DVBE) where space and time are continuous [23].

For free waves, where $\hat{k} = k_0$, we represent the discretization error by k_0 and find

$$\begin{aligned}\frac{\hat{\omega}}{\omega_0} &= 1 - \frac{k_0^2}{24}\left(1 - c_0^2\right) + \frac{k_0^4}{1920}\left(1 - 10c_0^2 + 9c_0^4\right) + O\left(k_0^6\right) \\ &\quad + i\frac{1}{2}(\omega_0\tau_\mathrm{v})\left[1 + \frac{k_0^2}{12}\left(3c_0^2 - 1\right) + O\left(k_0^4\right)\right] \\ &\quad + (\omega_0\tau_\mathrm{v})^2\left[\frac{1}{8}\frac{5c_0^2 - 1}{1 - c_0^2} + O\left(k_0^2\right)\right] + O((\omega_0\tau_\mathrm{v})^3).\end{aligned} \tag{25}$$

For the isothermal equation of state where $c_0^2 = c_\mathrm{vs}^2 = 1/3$ the second-order error in the lowest-order absorption disappears, a fact that has also been noted elsewhere [24].

While the free and forced wave results are similar at $O(k_0^2) = O(\omega_0^2)$ and at $O(\omega_0\tau_\mathrm{v})$, they differ elsewhere. The DVBE and Navier-Stokes fluid models agree up to $O(\omega_0\tau_\mathrm{v})$, but this DVBE does not agree at higher orders of $\omega_0\tau_\mathrm{v}$ with the Navier-Stokes model or higher-order fluid models such as the Burnett model [23].

V. APPLICATION TO NONLINEAR ACOUSTICS

The usefulness of this approach will now be demonstrated using the case of fully nonlinear acoustics, which requires the use of a nonlinear equation of state. In addition, this case will show that the neglected error terms are not relevant even for acoustically high Mach numbers.

There are two separate mechanisms of typically similar strength underlying nonlinear acoustics. First, a nonlinear equation of state gives a speed of sound that is higher in the wave peaks and lower in the wave troughs. For an ideal-gas plane wave, it results in a local speed of sound $c = c_0 + u(\gamma - 1)/2$, u being the local fluid velocity component of the wave [5,22]. Second, the fluid velocity component u of the sound wave causes an advection towards and against the propagation direction in peaks and troughs, respectively, augmenting the local wave propagation speed as $c + u$. These two effects together cause a total wave propagation speed $c + u = c_0 + u(\gamma + 1)/2$. This uneven wave propagation speed causes the waveform to distort into a shock wave.

Previous LB simulations of nonlinear acoustics [9,10] have only taken the second mechanism into account. Here we will also take the first mechanism into account by applying the isentropic equation of state (2).

Nonlinear plane-wave propagation can be modeled through the viscous Burgers equation, which can be derived from the conservation equations [22]. For an initially monofrequency free wave of frequency ω_0 and pressure amplitude $p^\star$, it becomes

$$\frac{\partial\bar{p}}{\partial\bar{t}} = \bar{p}\frac{\partial\bar{p}}{\partial\bar{t}_\mathrm{r}} + \bar{\alpha}_t\frac{\partial^2\bar{p}}{\partial\bar{t}_\mathrm{r}^2}, \tag{26}$$

where we have used the nondimensionalized parameters

$$\begin{aligned}\bar{p}(\bar{t}_\mathrm{r},\bar{t}) &= p'(\bar{t}_\mathrm{r},\bar{t})/p^\star, \quad \bar{t} = t/t_\mathrm{shock}, \\ \bar{t}_\mathrm{r} &= \omega_0 t - k_0 x, \quad \bar{\alpha}_t = \alpha_t t_\mathrm{shock}.\end{aligned} \tag{27}$$

Here the shock formation time

$$t_\mathrm{shock} = \frac{2\gamma}{\gamma+1}\frac{1}{\omega_0}\frac{p_0}{p^\star} \tag{28}$$

is defined as the time for the peak to catch up to the trough in the inviscid case and the physical absorption coefficient

$$\alpha_t = \frac{\omega_0^2}{2}\frac{\mu}{\rho_0 c_0^2}\left(\frac{4}{3} + \frac{\mu_\mathrm{B}}{\mu} + \frac{\gamma - 1}{\mathrm{Pr}}\right) \tag{29}$$

includes the dissipative effect of heat conduction in the last term through the adiabatic index γ and the Prandtl number Pr. While simple LB models do not simulate heat conduction, we can in general capture this dissipative effect by absorbing the heat conduction term into the bulk viscosity. In this simple one-dimensional case, we will match the simulation absorption coefficient (which is only affected by viscosity) with the

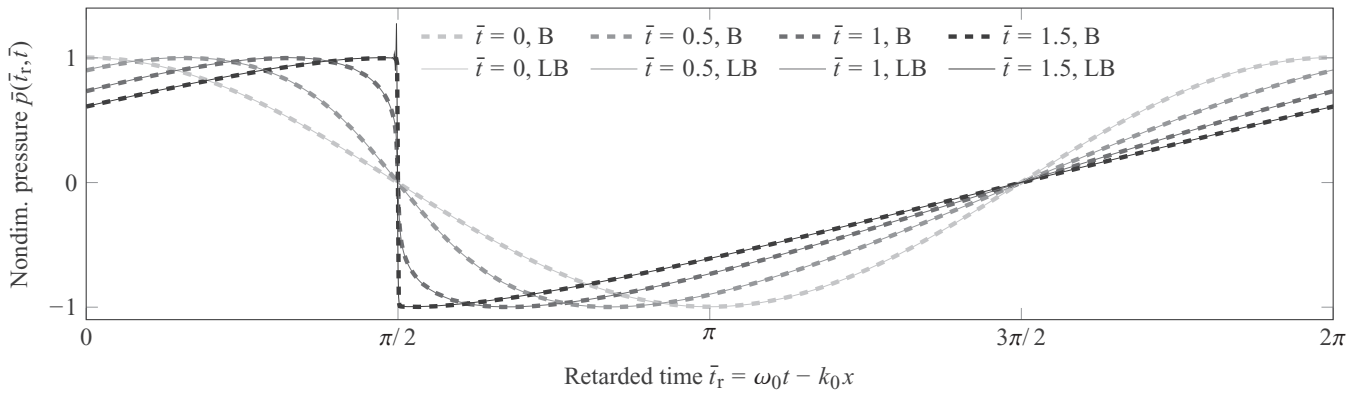

FIG. 1. Comparison of the LB simulation of nonlinear sound propagation (solid line) with a corresponding Burgers equation solution (dashed line) at various nondimensionalized times $\bar{t} = t/t_{\text{shock}}$. Note the spurious oscillation at the upper edge of the shock for $\bar{t} = 1.5$.

physical absorption coefficient (which is affected both by viscosity and heat conduction) by ensuring that they give the same absorption over a wave period.

For our physical case we choose a monatomic gas, where the dissipation is purely thermoviscous with $\mu_B = 0$ and there is no molecular relaxation. Such gases are characterized by $\gamma = 5/3$ and $\text{Pr} \simeq 2/3$ [27]. More specifically, we choose neon at the standard conditions $p_0 = 1.013 \times 10^5$ Pa and $T_0 = 300$ K. From the ideal gas law we find $\rho_{0,\text{ph}} = 0.820$ kg/m^3 and from (2) we find $c_{0,\text{ph}} = 454$ m/s. Its kinematic shear viscosity at these conditions is $\nu_{\text{ph}} = \mu_{\text{ph}}/\rho_{0,\text{ph}} = 3.89 \times 10^{-5}$ m^2/s [28].

We have here used the subscript "ph" to separate quantities in physical units from quantities in lattice units, denoted by the subscript "la." We link the two systems of units by the time and space resolutions Δt and Δx through the speed of sound $c_{0,\text{ph}} = c_{0,\text{la}} \Delta x/\Delta t$ and the absorption coefficient $(\alpha_t/\omega_0^2)_{\text{ph}} = (\alpha_t/\omega_0^2)_{\text{la}} \Delta t$. Consequently, the lattice shock formation time and the lattice wavelength are

$$t_{\text{shock,la}} = \frac{t_{\text{shock,ph}}}{\Delta t} = \frac{2\gamma}{\gamma+1} \frac{1}{\omega_{0,\text{ph}}} \frac{p_0}{p^\star} \frac{(1/c_{0,\text{la}^2} - 1)(\tau - 1/2)}{\left(\nu_{\text{ph}}/c_{0,\text{ph}}^2\right)[4/3 + \nu_B/\nu + (\gamma-1)/\text{Pr}]_{\text{ph}}}, \tag{30a}$$

$$\lambda_{\text{la}} = \frac{\lambda_{\text{ph}}}{\Delta x} = \frac{2\pi}{\omega_{0,\text{ph}}} \frac{(1/c_{0,\text{la}} - c_{0,\text{la}})(\tau - 1/2)}{\left(\nu_{\text{ph}}/c_{0,\text{ph}}^2\right)[4/3 + \nu_B/\nu + (\gamma-1)/\text{Pr}]_{\text{ph}}}, \tag{30b}$$

respectively. These equations correspond to the number of time steps required to form a shock and the required width of the system, respectively.

For the wave itself we choose a frequency of 10 kHz. Its Mach number is chosen as $\text{Ma} = u^\star/c_0 = 0.01$ as in [9]. The corresponding pressure amplitude is $p^\star/p_0 = \gamma \text{Ma}$.

Finally we choose the simulation parameters as $\tau = 0.6$ and $c_{0,\text{la}} = 0.95$. A high lattice speed of sound was chosen in order to both decrease the numerical dispersion as predicted by (25) and reduce the simulation time. This choice of $c_{0,\text{la}}$ includes a safety margin to ensure $c < 1$, as $c > 1$ would break the Courant-Friedrichs-Lewy (CFL) condition and destabilize the simulation. These choices result in $t_{\text{shock,la}} \simeq 29\,284$ and $\lambda_{\text{la}} \simeq 2331$.

The simulation is initialized in a periodic system of width λ_{la} using (20) and the eigenvector in (23). This initialization, based on the linearization analysis, is exact for an infinitesimally weak fluctuation. However, it is inexact for a stronger fluctuation; it causes a weak standing-wave effect since the initialized state contains a weak contribution from the mode for waves propagating in the opposite direction. Still, it remains more accurate than initializing with an equilibrium distribution given by linear Euler-level expressions for the density and fluid velocity of a wave, as done, e.g., in [9].

Snapshots of the simulation are shown from $\bar{t} = 0$ to 1.5 in Fig. 1 and are compared with a reference solution of the Burgers equation, which is found using the method of coupled ordinary differential equations [29] with $M = 600$ components and a fourth-order Runge-Kutta method with adaptive time steps. The two agree well up to at least $\bar{t} = 1$. For larger $\bar{t}$ a spurious oscillation develops at the upper edge of the shock in the LB solution. Such Gibbs-like phenomena generally occur when simulating shocks using dispersive numerical methods [30,31].

The different harmonic frequency components of the wave evolve as the shock develops. Higher harmonics feed on the lower ones, but are affected more heavily by absorption. Figure 2 shows the evolution of the amplitudes of the first six harmonics throughout the simulation. These were found by taking the spatial Fourier transform of the pressure in each time step. While these harmonics show excellent agreement with the harmonics of the Burgers equation solution, it is possible to discern a weak oscillation in the amplitude of the second harmonic due to the aforementioned standing-wave effect caused by the inexact method of initialization.

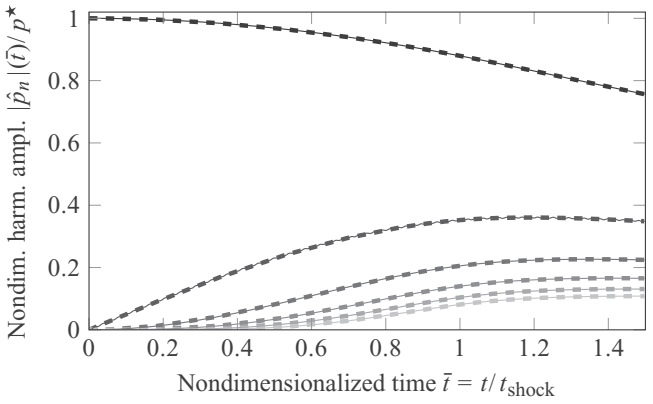

FIG. 2. Evolution of the amplitudes of the nth harmonics up to $\bar{t} = 1.5$ from the fundamental $n = 1$ (top, darkest line) to $n = 6$ (bottom, lightest line) for the LB simulation (solid line) and the Burgers equation (dashed line).

All things considered, the LB simulation results are in excellent agreement with the reference solution, proving that fully nonlinear acoustics can be simulated accurately with the LB method using an isentropic equation of state without any visible effect of the neglected error terms in the momentum equation (14).

VI. CONCLUSION

The isothermal equation of state of the simplest lattice Boltzmann method is insufficient in cases where the equation of state cannot be approximated as linear and constant. In this article we have reviewed the general requirements of equilibrium distributions $f_i^{(0)}$ that correctly recover a variable equation of state.

As has been stated previously [19], these requirements are not attainable for simple velocity sets. We have shown that the penalty of not fulfilling all the requirements are a number of additional error terms in the macroscopic momentum equation. The bulk viscosity error may be corrected [4,12,21] or avoided through a judicious choice of the speed of sound. The remaining error terms can be neglected using an analogous approximation scheme to the one used to derive the equations of nonlinear acoustics [22], though this further weakens the compressibility of the LB method.

One-dimensional problems can be simulated using the D1Q3 velocity set, where the equilibrium distribution $f_i^{(0)}$ is uniquely given by (17). The sound propagation properties of this equilibrium distribution were found for forced and free waves. These properties also hold for sound propagation along a main axis using a higher-dimensional velocity set [23]. However, the anisotropy of sound propagation could not be taken into account here, as it is individual to the different higher-dimensional velocity sets and equilibria.

The equilibrium distribution (17) was demonstrated through a simulation of nonlinear acoustics, with very good results. Both mechanisms of nonlinearity were simulated by using the isentropic equation of state. This improves on previous isothermal LB simulations of nonlinear acoustics [9,10], where only one of these mechanisms could be simulated.

A general equilibrium with variable equation of state should ideally be given in a form similar to (8) so that it could be applied to any simple velocity set. Some of the equilibria in the literature are defined only for specific velocity sets [15,18,19] and others [7,16,17] have not been proven to be stable in all simple velocity sets. Finding such an equilibrium that, like (8), can be applied directly to any simple velocity set while remaining provably stable is an important goal in the further investigation of this topic.

ACKNOWLEDGMENTS

The author would like to thank Paul J. Dellar and Jonas Lätt for very useful discussions on this topic.

[1] P. A. Thompson, *Compressible-Fluid Dynamics* (McGraw-Hill, New York, 1972).
[2] L. E. Kinsler, A. R. Frey, A. B. Coppens, and J. V. Sanders, *Fundamentals of Acoustics*, 4th ed. (Wiley, New York, 2000).
[3] S. Chen and G. D. Doolen, Annu. Rev. Fluid Mech. **30**, 329 (1998).
[4] P. J. Dellar, Phys. Rev. E **64**, 031203 (2001).
[5] D. T. Blackstock, *Fundamentals of Physical Acoustics* (Wiley, New York, 2000).
[6] X. Shan and H. Chen, Phys. Rev. E **47**, 1815 (1993).
[7] X. Shan and H. Chen, Phys. Rev. E **49**, 2941 (1994).
[8] A. L. Kupershtokh, D. A. Medvedev, and D. I. Karpov, Comput. Math. Appl. **58**, 965 (2009).
[9] J. M. Buick, C. L. Buckley, C. A. Greated, and J. Gilbert, J. Phys. A **33**, 3917 (2000).
[10] J. M. Buick and J. A. Cosgrove, J. Phys. A **39**, 13807 (2006).
[11] Y. H. Qian, D. d'Humières, and P. Lallemand, Europhys. Lett. **17**, 479 (1992).
[12] J. Lätt, Ph.D. thesis, University of Geneva, 2007.
[13] S. Ansumali, I. V. Karlin, and H. C. Öttinger, Europhys. Lett. **63**, 798 (2003).
[14] H. Yu and K. Zhao, Phys. Rev. E **61**, 3867 (2000).
[15] F. J. Alexander, H. Chen, S. Chen, and G. D. Doolen, Phys. Rev. A **46**, 1967 (1992).
[16] B. J. Palmer and D. R. Rector, J. Comput. Phys. **161**, 1 (2000).
[17] B. Chopard, A. Dupuis, A. Masselot, and P. O. Luthi, Adv. Complex Syst. **5**, 103 (2002).
[18] J. Tölke, M. Krafczyk, M. Schulz, and E. Rank, Philos. Trans. R. Soc. London Ser. A **360**, 535 (2002).
[19] P. J. Dellar, Phys. Rev. E **65**, 036309 (2002).
[20] T. F. Morse, Phys. Fluids **7**, 159 (1964).
[21] S. Bennett, Ph.D. thesis, King's College, Cambridge, 2010.
[22] M. F. Hamilton and C. L. Morfey, in *Nonlinear Acoustics*, edited by M. F. Hamilton and D. T. Blackstock (Academic, New York, 1998), Chap. 3, pp. 41–63.
[23] E. M. Viggen, Commun. Comput. Phys. **13**, 671 (2013).

[24] E. M. Viggen, Philos. Trans. R. Soc. London Ser. A **369**, 2246 (2011).
[25] E. M. Viggen, Phys. Rev. E **87**, 023306 (2013).
[26] C. Truesdell, J. Ration. Mech. Anal. **2**, 643 (1953).
[27] C. Cercignani, *The Boltzmann Equation and its Applications* (Springer, Berlin, 1988).
[28] E. Bich, J. Millat, and E. Vogel, J. Phys. Chem. Ref. Data **19**, 1289 (1990).
[29] J. H. Ginsberg and M. F. Hamilton, in *Nonlinear Acoustics* (Ref. [22]), Chap. 11, pp. 309–341.
[30] C. D. Levermore and J.-G. Liu, Physica D **99**, 191 (1996).
[31] J. Levesley, A. N. Gorban, and D. Packwood, in *Approximation Algorithms for Complex Systems*, edited by E. H. Georgoulis, A. Iske, and J. Levesley (Springer, Berlin, 2011), pp. 127–150.